

STATE-SELECTED PHOTODISSOCIATION DYNAMICS OF FORMALDEHYDE

C. BRADLEY MOORE
Department of Chemistry
University of California
Berkeley, California 94720

DOUGLAS J. BAMFORD
Chemical Physics Laboratory, SRI International
333 Ravenswood Avenue
Menlo Park, California 94025, USA

1. INTRODUCTION

The study of photofragmentation dynamics allows unimolecular chemical reactions to be examined in a state-resolved manner. Such state resolution can reveal a great deal about the potential energy surfaces which control these elementary events, and can serve as a crucial test for theories of reaction dynamics on those surfaces. The internal energy (v, J) distributions of photofragments have often been determined by laser-induced fluorescence, in cases where the fragments absorb in the visible or near-ultraviolet regions accessible with commercial tunable dye lasers^{1,2}. If the fragments do not have such convenient electronic spectra, the techniques of nonlinear optics must be used to provide the necessary sensitivity and spectral resolution. In the research presented here, such techniques have, for the first time, completely determined the distribution of energy among all the possible degrees of freedom in the photodissociation of a tetratomic molecule. In addition, rotational state resolution has been obtained in both entry and exit channels for the photofragmentation.

A. Experimental

To carry out state-selected photodissociation of formaldehyde followed by state-specific product detection of CO, two separate pulsed tunable laser systems were needed¹¹. The experimental concept was simple. The photolysis laser was tuned onto a formaldehyde absorption peak. A short time after the photolysis pulse, the probe laser was fired. The probe laser wavelength was then scanned to obtain a fluorescence excitation spectrum of the photochemical CO. Figure 2 shows the overall schematic.

Tunable ultraviolet radiation for state-selective formaldehyde photolysis was provided by a commercial system consisting of an excimer laser (Lumonics TE-861, 10 Hz, 15 ns) operating on XeCl at 308 nm which pumped a dye laser (Lambda-Physik 2002E). The dye laser was etalon-narrowed at 0.09 cm^{-1} bandwidth and pressure-tuned to produce tunable radiation in the 339 nm region. Formaldehyde absorption lines were identified by fluorescence excitation spectra¹⁵, using line lists provided by Ramsay¹⁶.

The vacuum ultraviolet probe laser system was patterned after

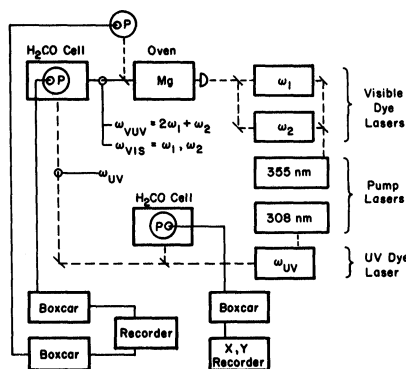


FIGURE 2 Schematic of photofragmentation experiment for $\text{CO}(v,J)$ measurements.

the original Toronto system¹⁷. The third harmonic of a Nd:YAG laser (Quanta-Ray DCR-1A) pumped two dye lasers. One of these lasers (Lambda-Physik 2002) was fixed at a wavelength of ~ 430.9 nm, corresponding to a two-photon resonance in magnesium (ω_1). The other (ω_2) dye laser (Quanta-Ray PDL-1) was tuned between 470 - 510 nm or between 565 - 600 nm, depending on the band of CO being studied. Energy from each of the dye lasers was typically 1.0 - 1.5 mJ per 5 ns pulse. The dye beams were combined in a Glan Prism and focused into the center of magnesium heat-pipe oven. Tunable VUV radiation ($\omega_8 = 2\omega_1 + \omega_2$) was generated in the focal region by resonantly enhanced four-wave mixing¹⁸. Carbon monoxide was excited via the $A^1\Pi \leftarrow X^1\Sigma^+$ transition¹⁹. Fluorescence at right angles to the plane of intersection of photolysis and probe lasers was detected by a solar-blind photomultiplier tube (EMR 542G-09-18). From spectra of room temperature CO, a detection limit of $\sim 10^8$ molecules per cm^3 per quantum state was inferred. Absolute pulse energies were not measured, but the observed CO detection efficiency corresponded to between 10^{11} and 10^{12} photons per pulse. To obtain a spectrum of the photochemical CO, the photolysis laser was tuned onto the desired formaldehyde absorption. Then, the lasers were synchronized to give a delay of 150 - 500 ns between photolysis and probe pulses. At the formaldehyde pressures of 0.05 - 0.10 Torr used, this was a sufficiently short delay to allow unrelaxed rotational distributions of CO to be obtained. The probe laser was then tuned to obtain a laser-induced fluorescence spectrum of the photochemical CO. A typical spectrum is shown in Fig.3.

B. Results

Carbon monoxide rotational distribution following H_2CO photolysis are shown in Figure 4. The CO has a remarkable amount of rotational excitation, with no detectable population in J states below 20. Room temperature CO, by contrast, has a rotational distribution

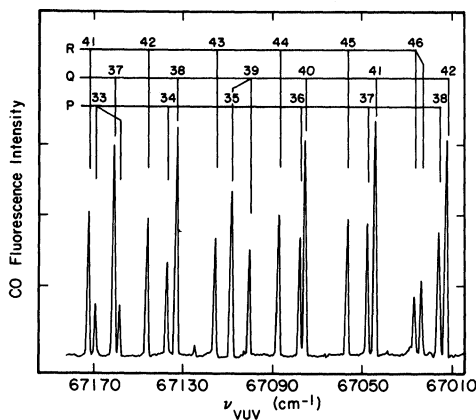


FIGURE 3 Portion of laser-induced fluorescence spectrum of carbon monoxide in the (2,0) band produced in the photolysis of 0.05 Torr of H_2CO , with the photolysis laser fixed on the $rQ_1(3)E + rQ_1(4)O$ transitions at 29515.2 cm^{-1} , and 150 ns delay (from Ref. 11, with permission).

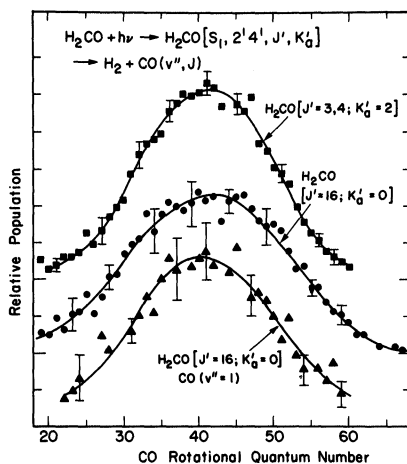


FIGURE 4 CO photofragment rotational distributions for H_2CO . Top trace is for $\text{CO}(v=0)$ produced by photolysis on the $rQ_1(3)E + rQ_1(4)O$ transitions of H_2CO . Pressure was

0.05 Torr and delay 150 ns. Middle trace is for CO($v=0$) produced by photolysis on the $pR_1(15)0$ transition of H_2CO at 29490.5 cm^{-1} . Conditions identical to those in the top trace. Bottom trace is for CO($v=1$) following $pR_1(15)0$ photolysis of 0.10 Torr of H_2CO , with 150 ns delay. The three traces have been displaced by 2 vertical units. The curves have all been normalized to the same area, with one vertical unit corresponding to a probability of 0.0178 for formation of a given J state of CO (from Ref. 11, with permission).

peaking at $J = 7$. CO ($v=1$) has nearly the same rotational distribution as CO($v=0$). The CO has very little vibrational excitation, in agreement with earlier infrared experiments⁹; no signals were seen for CO($v>1$). Figure 5 shows that increased rotational excitation of H_2CO leads to a slightly broader CO rotational distribution, without changing the most probable J value. As Figure 6 demonstrates, the CO rotational distribution cannot be characterized by a temperature.

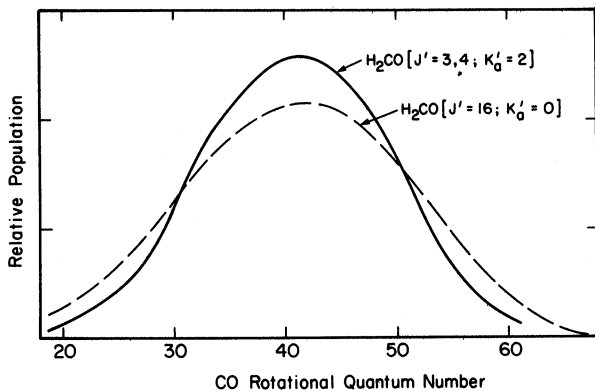


FIGURE 5 The effect of initial H_2CO angular momentum on the CO($v=0, J$) distribution. The hand-drawn lines through the data traces in the top two traces of Figure 4 show a broader distribution for the higher initial angular momentum (from Ref. 11, with permission).

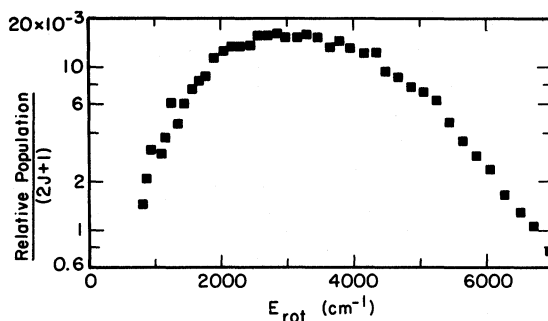


FIGURE 6 Boltzman plot for the data in the top trace of Fig. 4. The distribution cannot be characterized by a temperature (from Ref. 11, with permission).

3. HYDROGEN (v, J) DISTRIBUTION BY CARS SPECTROSCOPY

The vibrational and rotational distribution of the H_2 was determined using Coherent Anti-Stokes Raman Scattering (CARS), in a series of experiments carried out in France^{12,13}. The experimental concept was the same as that of the CO experiments described above, with the tunable VUV system replaced by the CARS spectrometer²⁰. The spectrometer has a detection limit for H_2 of approximately 10^{11} molecules per cm^3 per quantum state, making photolysis at the low pressures of formaldehyde used in the CO experiments impossible. Fortunately, it was observed that the (v, J) states of H_2 formed in formaldehyde photolysis have slow relaxation rates, so that distributions obtained from about 3 Torr of formaldehyde with 7 Torr of helium, with a 150 ns delay between photolysis and probe lasers were almost unrelaxed. The photolysis laser was a QuantaL YAG-pumped, frequency-doubled dye laser.

The complete (v, J) distribution following H_2CO photolysis at 29496 cm^{-1} is shown in Figure 7. The hydrogen has substantial vibrational and modest rotational excitation. Because the photolysis laser only excited formaldehyde molecules in odd K states (ortho-

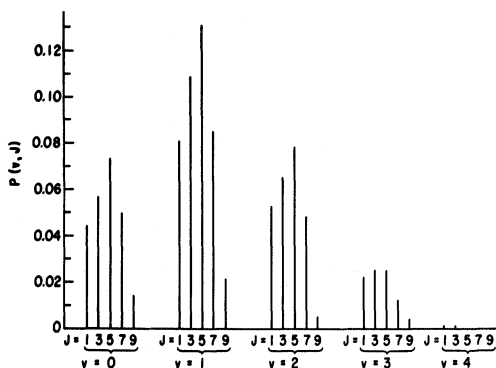


FIGURE 7 Quantum-state distribution for the $H_2(v,J)$ fragment from formaldehyde dissociation as determined by CARS spectroscopy (Ref. 13).

formaldehyde), only odd J states of H_2 (ortho-hydrogen) were produced, as earlier Raman experiments^{12,21} had demonstrated. Nuclear spin is conserved during the dissociation.

4. DISCUSSION

The available data can be combined to give a complete account of the energy disposal in this photodissociation. For each degree of freedom the experimental energy distribution is summarized in Table I.

Because the angular momentum of the CO is much larger than both the initial angular momentum of the H_2CO and the angular

TABLE I Energy distribution in $H_2CO \rightarrow H_2(v,J) + CO(v,J)$ as percent of 29500 cm^{-1} total energy.

| | Trans- lation | Rotation | | Vibration | |
|------------------------|------------------|----------|--------|-----------|-------|
| | | CO | H_2 | CO | H_2 |
| Minimum (10%) | 38 | 4(23) | 1/2(1) | 0(0) | 0(0) |
| Peak ($\Sigma = 97$) | 65 | 12(42) | 6(5) | 0(0) | 14(1) |
| Maximum | 91 | 22(58) | 10(7) | 7(1) | 40(3) |

Quantum numbers in parentheses.

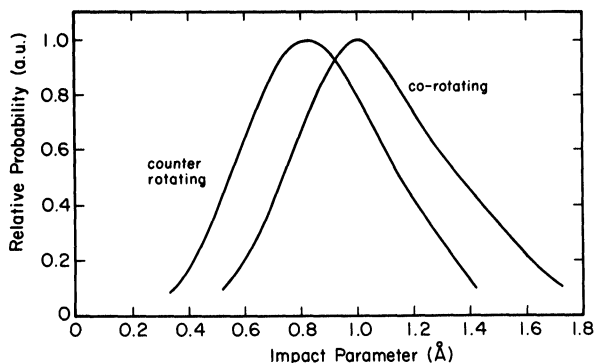


FIGURE 8 Calculated impact parameter distributions assuming uncorrelated (v,J) states of the two products. Because the distance from the carbon atom to the center of mass is $\sim 0.6 \text{ \AA}$ in both the transition state and the free CO molecule, most of the impact parameters correspond to a point of impact outside the carbon atom.

momentum of the H_2 product, the fragments must fly apart with a large amount of orbital angular momentum. The data presented above can be used, along with simple angular momentum conservation, to calculate a distribution function for the product impact parameter, b. The result is shown in Figure 8. In spite of the uncertainty about the relative directions of CO and H_2 rotation, the most probable impact parameter is clearly quite large, indicative of a bent transition state²² with the hydrogen having a point of impact a fraction of Angstrom outside the nucleus of the carbon atom.

5. CONCLUSION

The experimental characterization of the dynamics of formaldehyde photodissociation is now nearly complete. The use of well-established techniques of nonlinear optics has made this the most thoroughly studied and well-understood polyatomic photofragmentation. Application of these techniques to other problems in reaction dynamics will provide a sensitive test for both theoretical

potential energy surfaces and dynamical calculations using those surfaces.

REFERENCES

1. S. R. LEONE, Adv. Chem. Phys., 50, 255 (1982)
2. J. P. SIMONS, J. Phys. Chem., 88, 1287 (1984)
3. D. J. CLOUTHIER, D. A. RAMSAY, Ann. Rev. Phys. Chem., 34, 31 (1983)
4. C. B. MOORE, J. C. WEISSHAAR, Ann. Rev. Phys. Chem., 34, 525 (1983)
5. E. E. MARINERO, C. T. RETTNER, R. N. ZARE, A. H. KUNG, Chem. Phys. Lett., 95, 486 (1983)
6. E. E. MARINERO, R. VASUDEV, R. N. ZARE, J. Chem. Phys., 78, 692 (1983)
7. M. PEALAT, J.-P. E. TARAN, J. TAILLET, M. BACAL, A. M. BRUNETEAU, J. Appl. Phys., 52, 2687 (1981)
8. J. W. HEPBURN, F. J. NORTHRUP, G. L. OSRAM, J. C. POLANYI, J. M. WILLIAMSON, Chem. Phys. Lett., 85, 127 (1982)
9. P. L. HOUSTON, C. B. MOORE, J. Chem. Phys., 65, 757 (1976)
10. P. HO, D. J. BAMFORD, R. J. BUSS, Y. T. LEE, C. B. MOORE, J. Chem. Phys., 76, 3630 (1982)
11. D. J. BAMFORD, S. V. FILSETH, M. F. FOLTZ, J. W. HEPBURN, C. B. MOORE, J. Chem. Phys., 82, ... (1985)
12. M. PEALAT, D. DEBARRE, J.-M. MARIE, J.-P. E. TARAN, A. TRAMER, C. B. MOORE, Chem. Phys. Lett., 98, 299 (1983)
13. D. DEBARRE, M. LEFEBVRE, M. PEALAT, J.-P. E. TARAN, D. J. BAMFORD, C. B. MOORE (in preparation)
14. D. J. BAMFORD, Ph. D. Thesis, University of California, Berkeley, 1984.
15. J. C. WEISSHAAR, C. B. MOORE, J. Chem. Phys., 70, 5135 (1979)
16. D. A. RAMSAY (private communication).
17. J. W. HEPBURN, D. KLIMEK, K. LIU, R. G. MCDONALD, F. J. NORTHRUP, J. C. POLANYI, J. Chem. Phys., 74 6226 (1981)
18. S. C. WALLACE, G. ZDASIUK, Appl. Phys. Lett., 28, 449 (1976)
19. J. C. SIMONS, A. M. BASS, S. G. TILFORD, Astrophys. J., 155, 345 (1969)
20. S. DRUET, J.-P. E. TARAN, Progr. Quantum. Electron., 7, 1 (1981)
21. B. SCHRAMM, D. J. BAMFORD, C. B. MOORE, Chem. Phys. Lett., 98, 305 (1983)
22. J. D. GODDARD, Y. YAMAGUCHI, J. F. SCHAEFER, III, J. Chem. Phys. 75, 3459 (1981)